Dynamics of Plaque Formation in Alzheimer's Disease

B. Urbanc,* L. Cruz,* S. V. Buldyrev,* S. Havlin,*# M. C. Irizarry,§ H. E. Stanley,* and B. T. Hyman§

*Center for Polymer Studies and Department of Physics, Boston University, Boston, Massachusetts 02215 USA; #Gonda-Goldschmied Center and Department of Physics, Bar-Ilan University, Ramat-Gan, Israel; and §Neurology Service, Massachusetts General Hospital, Boston, Massachusetts 02114 USA

ABSTRACT Plaques that form in the brains of Alzheimer patients are made of deposits of the amyloid-β peptide. We analyze the time evolution of amyloid-β deposition in immunostained brain slices from transgenic mice. We find that amyloid-β deposits appear in clusters whose characteristic size increases from 14 μm in 8-month-old mice to 22 μm in 12-month-old mice. We show that the clustering has implications for the biological growth of amyloid-β by presenting a growth model that accounts for the experimentally observed structure of individual deposits and predicts the formation of clusters of deposits and their time evolution.

INTRODUCTION

Alzheimer's disease (AD) is a progressive neurodegenerative disorder of the central nervous system (Kandel et al., 1991), experienced by an increasing number of the elderly. AD is associated with plaques, which are primarily extracellular deposits of the amyloid-β (Aβ) peptide (40–42 amino acids long), which is derived from the larger amyloid precursor protein (APP). Although the role of plaques in AD is not understood (Beyreuther and Masters, 1997), compelling genetic and biochemical evidence suggests that Aβ is central to the pathological process in AD (Selkoe, 1994; Goate et al., 1991; Cai et al., 1993).

The physical and biological basis of Aβ aggregation is unknown. Unfortunately, experiments do not allow for a systematic study of the time development of plaques in AD patients because brain tissues can only be studied post mortem. The new technology of transgenic mice (Games et al., 1995), however, makes it possible to study temporal development of Aβ deposits in diseased brains because mice can be sacrificed at any stage of development. Fig. 1, *a* and *b*, present, respectively, two photomicrographs from brains of 8- and 12-month transgenic mice. The Aβ deposits (*dark connected areas* in Fig. 1) seem to cluster together into larger formations that typically consist of a larger deposit surrounded by many smaller ones. This is surprising because the distribution of APP throughout the cortex of transgenic mice is fairly uniform (Irizarry et al., 1997), and thus one would have expected a uniform spatial distribution of Aβ deposits at any stage of aggregation.

In this paper we focus on the time progression of Aβ aggregation and its implications for how Aβ forms in the brain. The question that we address in particular is why deposits are not uniformly distributed throughout the cortex but tend to be close to one another in clusters and what are the growth mechanisms (Vicsek, 1992; Herrmann, 1986; Takayasu, 1990; Meakin, 1998) that account for the observed spatial distribution of deposits. (In this paper we use the term "cluster" to mean not a connected entity (as usually used), but rather a correlated yet unconnected set of objects (e.g., a galaxy).) The conclusions of the paper will be stated in terms of the time evolution of the deposits and the clusters of deposits.

To quantify the experimentally observed clusters of deposits and their time evolution (Fig. 1, *a* and *b*), we examine photomicrographs from the temporal neocortex and hippocampus of transgenic mice at 8 and 12 months of age and calculate the correlation function, $C(r)$, between deposits. By definition, $C(r)$ is proportional to the probability of finding the center of mass of a deposit at a given distance r from a reference deposit at $r = 0$. In practice, we determine $C(r)$ by first identifying the center of mass for each connected region (deposit) and then calculating the histogram of distances between pairs of deposits. $C(r)$ is normalized so that it approaches the average number density of deposits at large distances r. Results for the average $\langle C(r) \rangle$ are presented in Fig. 2, *a* and *b* (*solid lines*) for all photomicrographs from 8- and 12-month mice, respectively.

As a control we randomly shuffle the deposits by placing a disk with the area of the initial deposit in place of the original deposit, and then randomize the positions of the disks in a nonoverlapping way. For the control case, $\langle C(r) \rangle$ (*dashed lines* in Fig. 2, *a* and *b*) is constant (noncorrelated) everywhere except at very small distances, where it decreases because of the exclusion area of the deposits.

From inspection of Fig. 2, *a* and *b*, we see that $\langle C(r) \rangle$ shows a dramatically increased probability for finding a deposit at small r, in comparison to $\langle C(r) \rangle$ for the shuffled controls. This means that we can define ξ_{cl}, the characteristic size of clusters, as the size where $\langle C(r) \rangle$ reaches the

Received for publication 23 September 1998 and in final form 15 December 1998.

Address reprint requests to Dr. H. E. Stanley, Center for Polymer Sciences, Department of Physics, Boston University, 590 Commonwealth Ave., Boston, MA 02215. Tel.: 617-353-2617; Fax: 617-353-3783; E-mail: hes@bu.edu.

Dr. Urbanc is on leave from the J. Stefan Institute, Jamova 39, 1001 Ljubljana, Slovenia.

0006-3495/99/03/1330/05 $2.00

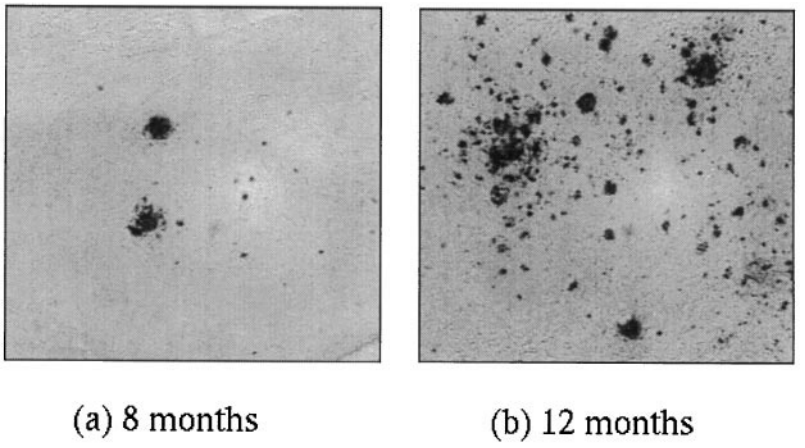

FIGURE 1 Images taken with an optical microscope, of samples of PDAPP transgenic mice (Games et al., 1995) at ages of (*a*) 8 months and (*b*) 12 months (magnification 16×, size 100 μm × 100 μm, depth 50 μm). A prominent feature of the upper left quadrant of *b* is a large cluster formed by many smaller deposits. Sections were immunostained for Aβ using antibody 10D5 (Hyman et al., 1993).

value of $\langle C(r)\rangle$ for shuffled controls. For mice at age 8 months, the curves join at about $\xi_{cl} = 14$ μm, whereas for mice at age 12 months, ξ_{cl} is increased to 22 μm. To confirm the results from $\langle C(r)\rangle$, we determine ξ_{cl} of each $C(r)$ calculated from an individual photomicrograph. Histograms of individual ξ_{cl} (Fig. 2 *c*) show peaks at 14 μm and 22 μm for 8-month and 12-month mice, respectively.

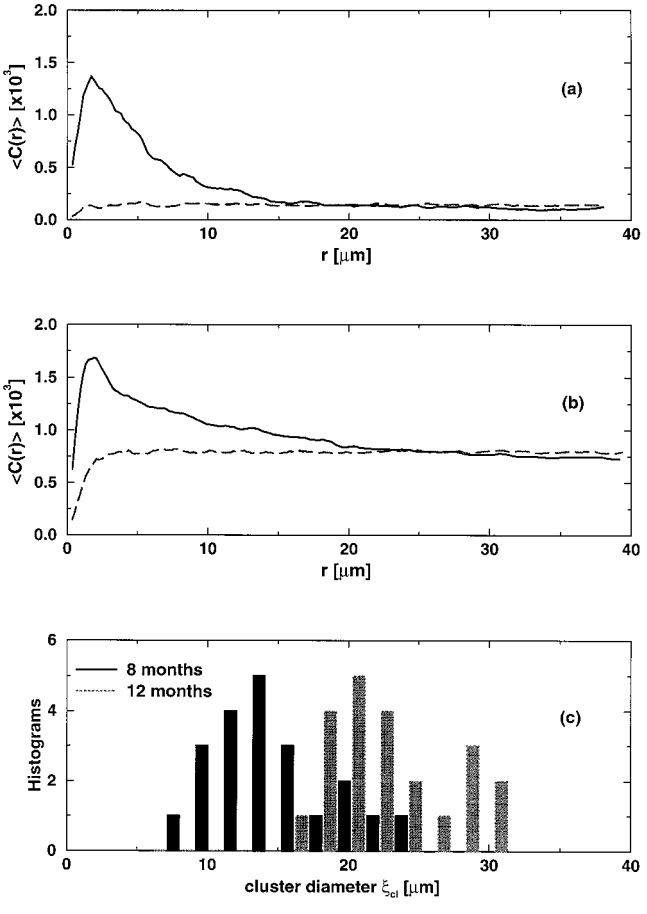

FIGURE 2 Solid lines represent the $\langle C(r)\rangle$ of deposits from transgenic mice at ages of (*a*) 8 months (21 micrographs) and (*b*) 12 months (22 micrographs). Dashed lines are the corresponding $\langle C(r)\rangle$ from the shuffled controls. (*c*) Histograms of cluster sizes extracted from each $\langle C(r)\rangle$ corresponding to individual micrographs.

The natural question that follows is: How does ξ_{cl} increase in time? One possible mechanism is that the clusters grow (ξ_{cl} increases) because the deposits that form them grow. We show that this is not the case and that instead the deposits—whose characteristic size does not change with time—cluster together, increasing ξ_{cl}. To show this, we calculate ξ_{dep}, the characteristic size of deposits, by first calculating the average deposit area B from the size distribution of deposit areas and then computing $\xi_{dep} = 2\sqrt{B/\pi}$. We find $\xi_{dep} \approx 1.3 \pm 0.5$ μm for both the 8- and 12-month mice. This result is in accord with the observation that the typical diameter of an Aβ deposit in AD brain does not vary as the illness progresses (Arriagada et al., 1992; Hyman et al., 1995). Because ξ_{dep} does not change in time and ξ_{cl} increases from $\sim 11 \times \xi_{dep}$ in 8-month mice to $\sim 17 \times \xi_{dep}$ in 12-month mice (Fig. 2, *a* and *b*), we conclude that clusters grow because more deposits cluster together.

To study the implications of the above results for Aβ aggregation, we propose a phenomenological model that is based on several experimental findings. From earlier studies we know that a successful model of the experimentally determined size distribution of Aβ has to consider growth that is proportional to the volume of the growing aggregate (Hyman et al., 1995). Further work that revealed the porosity of individual Aβ deposits, using confocal microscopy (Cruz et al., 1997), clarified that the model should take into account disaggregation, which competes with aggregation, as well as surface diffusion. (For a deposit to acquire a typical porous structure with well-defined pores, the model additionally takes into account surface diffusion—after every step each particle in the lattice is allowed to move to one randomly chosen neighboring empty site only if the new position has more nearest-neighboring particles. However, the model does not need surface diffusion to exhibit the clustering and its further time evolution, as presented in this paper.) Starting from these elements, the challenge is to test the time evolution of the model against the experimental results of Aβ deposition.

The model is defined as follows. Starting from a random arrangement of occupied sites (particles) in a discrete three-dimensional lattice, each particle is chosen with equal probability 0.5 to duplicate or to be eliminated. This initial state of randomly distributed "seeds" corresponds to the fact that APP is uniformly distributed throughout the cortex (Irizarry et al., 1997), and therefore the growth of deposits is equally probable at any position. Furthermore, a particle chosen to duplicate (aggregation) will do so with probability P_{agg}, and, if chosen to be eliminated (disaggregation), it is removed with probability P_{dis}. In the aggregation process, a newly created particle performs a random walk from the original occupied site until the first empty site is encountered. This yields a growth proportional to the volume in agreement with experimental data (Hyman et al., 1995). The equation for an average number of particles (fluctuations due to a probabilistic nature of the model are not taken into account), N_{t+1}, at time $t + 1$ is

$$N_{t+1} = N_t + \frac{1}{2}(P_{agg} - P_{dis})N_t \tag{1}$$

The two probabilities P_{agg} and P_{dis} can easily be interpreted as the aggregation and disaggregation rates, respectively. If both P_{agg} and P_{dis} are kept constant, Eq. 1 yields either exponential growth (if $P_{agg} > P_{dis}$) or exponential decrease (if $P_{agg} < P_{dis}$) of the number of particles. This model can be mapped onto percolation on the Cayley tree lattice (Harris, 1989). Even for $P_{agg} = P_{dis}$, the fluctuations eventually lead to the extinction of particles because the probability that the descendants of any given particle survive until time step t decreases as $1/\sqrt{t}$. Because in the brain of AD patients a relatively fixed percentage of cortical surface area is covered by Aβ deposits regardless of duration or severity of dementia (no exponentially unstable behavior), we postulate a steady state. (Aβ can occupy as much as 15–20% of the surface area of the cortex of the AD brain; see, e.g., Arriagada et al. (1992) and Hyman et al. (1993, 1995).) To achieve a dynamic steady state in the model, we introduce a feedback that acts upon the disaggregation process such that at every time step, P_{dis} is changed in proportion to the change in the coverage N_t/V (where V is the total number of sites in the lattice). Hence

$$P_{dis}(t + 1) = P_{dis}(t) + w\frac{N_t - N_{t-1}}{V}, \tag{2}$$

where $w > 0$ parameterizes the feedback strength. The feedback mechanism as introduced here postulates a global response of the brain: a change in the disaggregation rate due to the change in the overall amount of Aβ. This response is such that it tends to minimize the changes occurring in the brain, thus naturally leading to a steady state. At this point the model is defined completely.

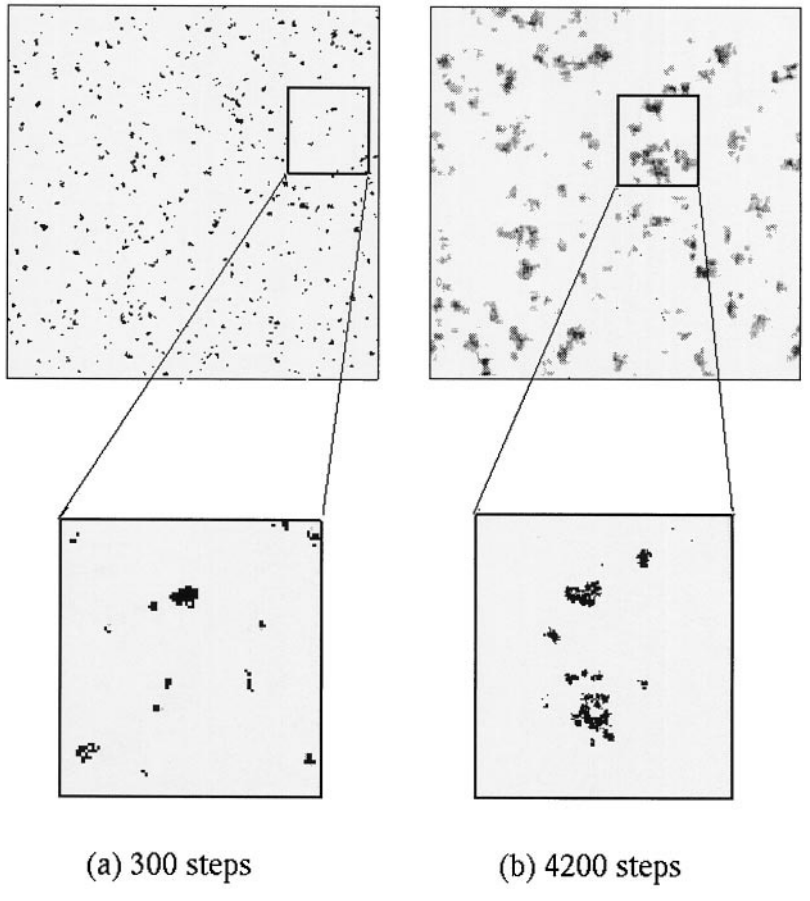

FIGURE 3 Snapshots from the growth model simulation after (*a*) 300 and (*b*) 4200 steps with two magnified inserts. The simulation, on a lattice of size 512 × 512 × 32, is started with 2.5% of scattered sites occupied. The aggregation and disaggregation probabilities are $P_{agg} = P_{dis} = 0.80$. Although surface diffusion is not needed for the model to exhibit the clustering, we use in this simulation a surface diffusion corresponding to 10 relaxation steps per particle at every time step.

Some remarks about the above two equations are in order. The equation for the average number of particles in the model with feedback is defined by Eq. 1, with $P_{dis} = P_{dis}(t)$, as given by Eq. 2. The solution of the combined recurrent Eqs. 1 and 2 can be found by numerical iterations. However, by approximating the differences in both equations by first derivatives (thus neglecting the time delays), we can find an analytic solution that is fairly close to the exact one. From Eq. 2 we first find P_{dis} to be a linear function of N_t, then we insert the solution $P_{dis}(t)$ into Eq. 1, solve it for N_t, and find

$$N_t = \frac{N_\infty}{1 + [(N_\infty - N_0)/N_0] \exp(-At)}, \quad (3)$$

where $N_0 = N_{t=0}$ is the number of initial "seeds," $N_\infty = N_0 + V(P_{agg} - P^0_{dis})/w$ is the steady-state number of particles as $t \to \infty$ (total coverage), which depends only on the initial conditions (N_0 and $P^0_{dis} = P_{dis}(t = 0)$), and $A = [P_{agg} - P^0_{dis} + wN_0/V]/2$ is the rate of approaching the steady state. How do we understand this solution? Let us say that the deposition starts with a small number of seeds (small N_0) randomly placed in the lattice and assume that $P^0_{dis} = 0$ (no disaggregation initially). Then N_t (the total amount of deposited Aβ) will keep increasing with t as well as P_{dis} until $P_{dis}(t)$ is equal on average to P_{agg}. At the same time that $P_{dis}(t)$ stabilizes, the total number of particles N_t saturates as well, and the system is in a dynamic steady state. The necessity of disaggregation and feedback processes in the model highlights the importance of biological modifiers (e.g., feedback clearance mechanisms such as microglia; Paresce et al., 1996; El-Khoury, 1996) in shaping the topology and microarchitecture of Aβ deposits.

We now proceed to test the model by examining whether it provides insight into the clustering phenomenon and whether it is also able to explain the time dependence of Aβ deposition. Fig. 3, with the two magnified insets, shows the time evolution of our simulation (to be compared with Fig. 1). Within the time scale of 300 steps the deposits form. The clustering of deposits, however, is not very pronounced until the time that is roughly one order of magnitude larger, i.e., around 4000 steps. At 4200 steps (Fig. 3 *b*), well-defined clusters occupy an area that is small compared to the system size and that depends on the total number of occupied sites in the lattice (Meyer et al., 1996). As time progresses the model predicts typically big deposits that are surrounded by many smaller ones, thus forming clusters similar to the ones observed in transgenic mice.

As in the experiment, we quantify the degree of clustering in the model by considering cross sections from the simulations at different times (up to 4200 simulation steps) and calculating $\langle C(r) \rangle$ (Fig. 4, *a* and *b*, with corresponding shuffled controls). As in the experimental case, $\langle C(r) \rangle$ increases at small r. Furthermore, ξ_{cl} increases with time (Fig. 4 *c*), in agreement with the results of the analysis of photomicrographs of transgenic mice at age 8 and 12 months. On the other hand, ξ_{dep} reaches a saturation value on the time scale of 1000 steps, whereas ξ_{cl} continues to increase

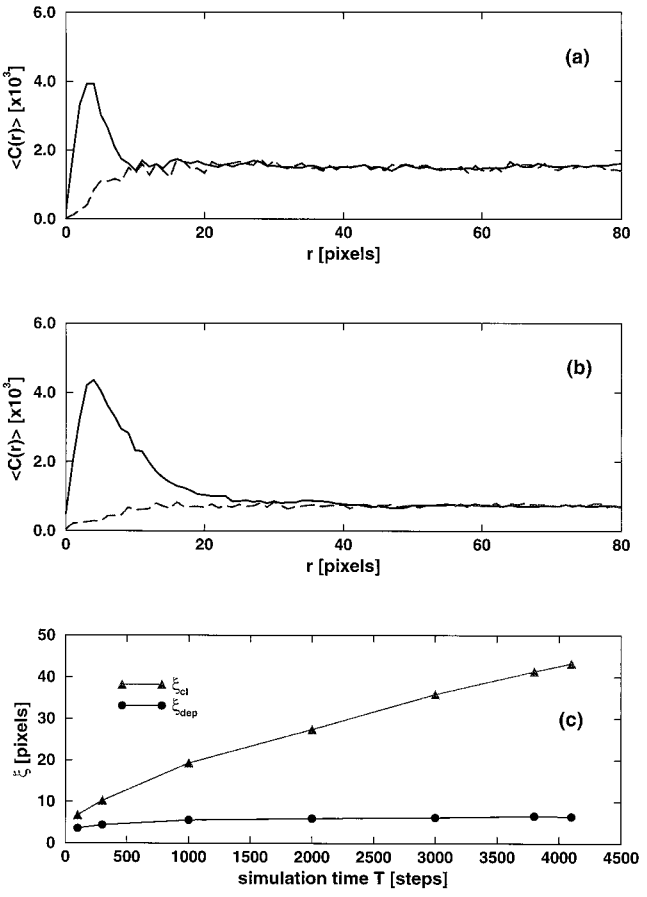

FIGURE 4 Solid lines represent $\langle C(r) \rangle$ averages over 16 different cross sections of the simulation, and dashed lines represent the corresponding averages $\langle C(r) \rangle$ of the shuffled controls after (*a*) 300 and (*b*) 4200 simulation steps. (*c*) Time dependence of the characteristic deposit size ξ_{dep} and the characteristic cluster size ξ_{cl} as predicted by the model.

beyond 4000 steps (compare the two curves in Fig. 4 *c*). The model therefore predicts that after ~3000 steps the deposits of fixed sizes assemble into clusters, and the size of clusters, ξ_{cl}, increases with time, in agreement with the experimental observations above.

The increase in ξ_{cl} can be understood within the model by considering the asymmetry between aggregation and disaggregation (Meyer et al., 1996). We know that in the dynamic equilibrium the average disaggregation rate, $\langle P_{dis} \rangle$, is equal to the aggregation rate, P_{agg}, which means that equal amounts of particles, on average, are created and destroyed. Let us consider the symmetrical case first. If the growth rule would allow the duplicate particle to appear at any empty site in the lattice, the distribution of particles would be uniform and independent of time, and neither deposits nor clusters would form. The asymmetry in our model is attained because the duplicate particle occupies the nearest empty site it encounters, whereas the disaggregation is uniform (independent of the position). This asymmetry thus permits small deposits to occur only very close to a big deposit. As time progresses, the asymmetry leads to a higher effective disaggregation probability for particles that are

isolated and far from the big deposit, as opposed to the particles close to it.

The experimental part of our analysis leads to the following conclusions. Aβ deposits in the brains of transgenic mice are not randomly distributed throughout the cortex as expected. Rather, they appear in clusters whose characteristic size increases with the duration of the illness. This study sheds light on the evolution of Aβ deposits from the initially uniformly distributed APP. In the second part we give an interpretation of the observed clustering in transgenic mice within the phenomenological model, which has strong implications for the understanding of pathological changes in Alzheimer's disease. Previously, diffuse, amorphous amyloid deposits observed in the brain of Alzheimer patients have been called "primitive" or "immature" plaques, implying that they "mature" into compact classical senile plaques later in the disease process (Terry and Davies, 1980). Our phenomenological model, data from transgenic mice, and preliminary results from human AD cases argue against this paradigm and instead suggest that the amorphous deposits are not the direct precursor of the more compact senile plaques seen later in the disease. Instead, the model predicts the time evolution of the morphological appearance of Aβ deposits from smaller to bigger clusters of plaques. Moreover, the model presented here supports the idea that Aβ deposition may be a reversible process, with aggregation and disaggregation as its essential components, a feature of critical importance for therapeutic strategies aimed at resolving Aβ deposition.

We thank Drs. Dora Games and Dale Schenk, Athena Neurosciences, for providing the PDAPP mouse tissue used in this work. We also appreciate helpful discussions with T. Gómez-Isla, R. Knowles, M. R. Sadr-Lahijany, D. Wolf, and C. Wyart.

This paper was partly supported by National Institutes of Health grant AG08487, the National Science Foundation, and the Adler Foundation.

REFERENCES

Arriagada, P. V., J. H. Growdon, E. T. Hedley-Whyte, and B. T. Hyman. 1992. Neurofibrillary tangles but not senile plaques parallel duration and severity of Alzheimers disease. *Neurology.* 42:631–639.

Beyreuther, K., and C. L. Masters. 1997. Alzheimer's disease: the ins and outs of amyloid-β. *Nature.* 389:677–678.

Cai, X.-D., T. E. Golde, and S. G. Younkin. 1993. Release of excess amyloid β in protein from a mutant amyloid β-protein precursor. *Science.* 259:514–516.

Cruz, L., B. Urbanc, S. V. Buldyrev, R. Christie, T Gómez-Isla, S. Havlin, M. McNamara, H. E. Stanley, and B. T. Hyman. 1997. Aggregation and disaggregation of senile plaques in Alzheimer disease. *Proc. Natl. Acad. Sci. USA.* 94:7612–7616.

El-Khoury, J. 1996. Scavenger receptor-mediated adhesion of microglia to β-amyloid fibrils. *Nature.* 382:716–719.

Games, D., D. Adams, R. Alessandrini, R. Barbour, P. Berthelette, C. Blackwell, T. Carr, J. Clemens, T. Donaldson, F. Gillespie, T. Guido, S. Hagoplan, K. Johnson-Wood, K. Khan, M. Lee, P. Leibowitz, I. Lieberburg, S. Little, E. Masliah, L. McConlogue, M. Montoya-Zavala, L. Mucke, L. Paganini, E. Penniman, M. Power, D. Schenk, P. Seubert, B. Snyder, F. Soriano, H. Tan, J. Vitale, S. Wadsworth, B. Wolozin, and J. Zhao. 1995. Alzheimer-type neuropathology in transgenic precursor protein mice overexpressing V717F b-amyloid precursor protein. *Nature.* 373:523–527.

Goate, A., M.-C. Chartier-Harlin, and M. Mullan. 1991. Segregation of a missense mutation in the amyloid precursor protein gene with familial Alzheimer's disease. *Nature.* 349:704–707.

Harris, T. E. 1989. The Theory of Branching Processes. Dover Publications, New York.

Herrmann, H. J. 1986. Geometrical cluster growth models and kinetic gelation. *Phys. Rep.* 136:153–227.

Hyman, B. T., K. Marzloff, and P. V. Arriagada. 1993. The lack of accumulation of senile plaques or amyloid burden in Alzheimers disease suggests a dynamic balance between amyloid deposition and resolution. *J. Neuropathol. Exp. Neurol.* 52:594–600.

Hyman, B. T., H. L. West, G. W. Rebeck, S. V. Buldyrev, R. N. Mantegna, M. Ukleja, S. Havlin, and H. E. Stanley. 1995. Quantitative analysis of senile plaques in Alzheimer disease: observation of log-normal size distribution and of differences associated with apolipoprotein E genotype and trisomy 21 (Down syndrome). *Proc. Natl. Acad. Sci. USA.* 92:3586–3590.

Irizarry, M. C., F. Soriano, M. McNamara, K. J. Page, D. Schenk, D. Games, and B. T. Hyman. 1997. A beta deposition is associated with neuropil changes, but not with overt neuronal loss in the human amyloid precursor protein V717F (PDAPP) transgenic mouse. *J. Neurosci.* 17: 7053–7059.

Kandel, E. R., J. H. Schwartz, and T. M. Jessel, eds. 1991. Principles of Neural Science. Appleton and Lange, Norwalk, CT.

Meakin, P. 1998. Fractals, Scaling and Growth Far from Equilibrium. Cambridge University Press, Cambridge.

Meyer, M., S. Havlin, and A. Bunde. 1996. Clustering of independently diffusing individuals by birth and death processes. *Phys. Rev. E.* 54: 5567–5570.

Paresce, D., R. Ghosh, and F. R. Maxfield. 1996. Microglial cells internalize aggregates of the Alzheimer's disease amyloid beta-protein via a scavenger receptor. *Neuron.* 17:553–565.

Selkoe, D. 1994. Alzheimer's disease: a central role for amyloid. *J. Neuropathol. Exp. Neurol.* 53:438–447.

Takayasu, H. 1990. Fractals in the Physical Sciences. Manchester University Press, Manchester.

Terry, R. D., and P. Davies. 1980. Dementia of the Alzheimer type. *Annu. Rev. Neurosci.* 3:77–95.

Vicsek, T. 1992. Fractal Growth Phenomena, 2nd Ed. World Scientific, New York.